

Cite this: *CrystEngComm*, 2011, **13**, 5321

www.rsc.org/crystengcomm

## COMMUNICATION

Solvent-induced 1,3-*N,S*- vs. 1,5-*S,S'*-coordination in the Ni<sup>II</sup> complex [Ni{*p*-Me<sub>2</sub>NC<sub>6</sub>H<sub>4</sub>NHC(S)NP(S)(*OiPr*)<sub>2</sub>}<sub>2</sub>]<sup>†</sup>Maria G. Babashkina,<sup>\*a</sup> Damir A. Safin,<sup>a</sup> Monika Srebro,<sup>b</sup> Piotr Kubisiak,<sup>b</sup> Mariusz P. Mitoraj,<sup>\*b</sup> Michael Bolte<sup>c</sup> and Yann Garcia<sup>a</sup>

Received 30th March 2011, Accepted 16th June 2011

DOI: 10.1039/c1ce05387f

Reaction of the deprotonated *N*-thiophosphorylated thiourea *p*-Me<sub>2</sub>NC<sub>6</sub>H<sub>4</sub>NHC(S)NHP(S)(*OiPr*)<sub>2</sub> (HL) with NiCl<sub>2</sub> leads to violet [Ni(L-1,3-*N,S*)<sub>2</sub>] or dark violet [Ni(L-1,5-*S,S'*)<sub>2</sub>]·(CH<sub>3</sub>)<sub>2</sub>C=O crystals that were isolated by recrystallization from a mixture of CH<sub>2</sub>Cl<sub>2</sub> or acetone, respectively, and *n*-hexane.

In the literature there is a number of Ni<sup>II</sup> complexes with the imidodiphosphinate ligands R<sub>2</sub>P(X)NP(Y)R'<sub>2</sub> (IDP) (X, Y = O, S, Se, Te)<sup>1</sup> and acylthioamides RC(S)NC(X)R' (AA) or aroylthioureas R<sub>2</sub>NC(S)NC(X)R' (ATU) (X = O, S).<sup>2</sup> These complexes are of great interest due to their structural versatility (square-planar, octahedral, tetrahedral). However, the chelate backbones of the IDP, AA and ATU ligands are coordinated to the Ni<sup>II</sup> cation through the donor X and Y atoms.

The synthesis and complexation properties of *N*-(thio)phosphorylated thioamides and thioureas RC(S)NHP(X)(OR')<sub>2</sub> (X = O, S) (NTT), which are IDP's, AA's and ATU's asymmetrical analogues, have been extensively studied,<sup>3</sup> but there is still limited information about the structures of Ni<sup>II</sup> complexes with NTT. In previous contributions we have also studied the structures of Ni<sup>II</sup> complexes with NTT (X = O) ligands and demonstrated that their square planar complexes with Ni<sup>II</sup> exhibit either a 1,3-*N,S*- or a 1,5-*O,S* coordination mode. It was established, that intramolecular hydrogen bonds N-H...O=P are a necessary condition for the formation of 1,3-*N,S*-isomers for R = PhNH, *p*-MeOC<sub>6</sub>H<sub>4</sub>NH, *p*-BrC<sub>6</sub>H<sub>4</sub>NH, *iPr*NH, *t*BuNH, *cyclo*-C<sub>6</sub>H<sub>11</sub>NH, 1-AdNH, (4'-benzo-15-crown-5)NH;<sup>4</sup> whereas 1,5-*O,S* coordination takes place when H-bonding in the coordinated anionic ligands is not possible (R = Et<sub>2</sub>N, morpholine-*N*-yl<sup>5</sup>). Moreover, *N*-phosphorylated thioamides RC(S)NHP(O)(*OiPr*)<sub>2</sub> (R = *p*-BrC<sub>6</sub>H<sub>4</sub>, Ph<sup>6</sup>) form distorted octahedral complexes

with Ni<sup>II</sup>, where two deprotonated ligands are coordinated through the sulfur and oxygen atoms of the C=S and P=O groups, respectively, and two neutral forms of the ligands are bonded through the oxygen atoms of the P=O groups. Furthermore, the 1,3-*N,S*-coordination of the NTT (X = O) ligands towards Ni<sup>II</sup> allows one to obtain octahedral complexes by the reaction with additional donor ligands such as 2,2'-bipyridine and 1,10-phenanthroline.<sup>4e</sup> It is important to note, that the situation for the coordination of Ni<sup>II</sup> to the NTT ligands is further complicated by the possibility to form tetrahedrally configured complexes as recently described for the complexes [Ni{R<sub>2</sub>NC(S)NP(S)(*OiPr*)<sub>2</sub>}<sub>2</sub>] (R = Me, H), which in polar solvents exhibit spectral features for a tetrahedral complex (colour, paramagnetism), while in non-polar solvents and in the solid state the complex has a *trans* square planar geometry. Both configurations clearly exhibit a 1,5-*S,S'*-coordination.<sup>6</sup> Recently we reported the first example of a 1,5,7-*N,N',S*-coordination of the deprotonated chelate backbone in the square planar Ni<sup>II</sup> complex [Ni{2-Py(6-Me)NHC(S)NP(S)(*OiPr*)<sub>2</sub>}<sub>2</sub>]. No crystal structure could be obtained so far, but from the spectroscopic results it is clear, that the 2-pyridyl functions are additionally coordinating in this octahedral complex.<sup>7</sup> As a preliminary result we have also reported a first success to induce the formation of a 1,3-*N,S*-coordination mode in the *trans* square planar Ni<sup>II</sup> complex with the dithio-containing NTT ligands.<sup>8</sup>

In this work, we describe the synthesis of new Ni<sup>II</sup> complexes with the *N*-thiophosphorylated thiourea *p*-Me<sub>2</sub>NC<sub>6</sub>H<sub>4</sub>NHC(S)NHP(S)(*OiPr*)<sub>2</sub> (HL). In order to obtain a complete picture of the electronic structures of the complexes we carried out DFT calculations on the structures focusing on the energy difference between [Ni(L-1,3-*N,S*)<sub>2</sub>], [Ni(L-1,5-*S,S'*)<sub>2</sub>] and [Ni(L-1,5-*S,S'*)<sub>2</sub>]·(CH<sub>3</sub>)<sub>2</sub>C=O conformers. Finally, we investigated the molecular structures of the complexes in solutions by multinuclear NMR and UV-Vis absorption spectroscopy. The latter method, in combination with electrochemical investigations (cyclic voltammetry) should also allow us to shed light on the electronic properties of these isomers.

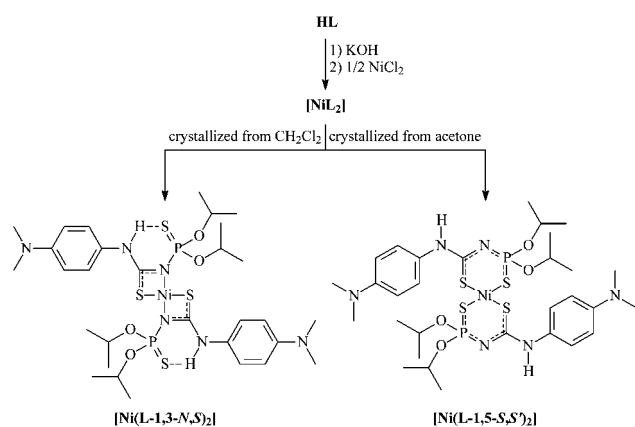
The raw material [NiL<sub>2</sub>] was prepared by the following procedure: the ligand was deprotonated *in situ* using KOH, followed by reaction with NiCl<sub>2</sub> (Scheme 1, see also ESI<sup>†</sup>). The obtained dark violet solid material is soluble in most polar solvents. Violet [Ni(L-1,3-*N,S*)<sub>2</sub>] or dark violet [Ni(L-1,5-*S,S'*)<sub>2</sub>]·(CH<sub>3</sub>)<sub>2</sub>C=O crystals were isolated by recrystallization from a 1 : 5 mixture of CH<sub>2</sub>Cl<sub>2</sub> or acetone, respectively, and *n*-hexane. It is noteworthy, that according to the IR

<sup>a</sup>Institute of Condensed Matter and Nanosciences, MOST - Inorganic Chemistry, Université Catholique de Louvain, Place L. Pasteur 1, 1348 Louvain-la-Neuve, Belgium. E-mail: maria.babashkina@ksu.ru; Fax: +32(0) 1047 2330; Tel: +32(0) 1047 2831

<sup>b</sup>Department of Theoretical Chemistry, Jagiellonian University, R. Ingardena 3, 30-060 Cracow, Poland. E-mail: mitoraj@chemia.uj.edu.pl

<sup>c</sup>Institut für Anorganische Chemie J.-W.-Goethe-Universität, Frankfurt/Main, Germany

<sup>†</sup> Electronic supplementary information (ESI) available. CCDC reference numbers 805250 and 814216. For ESI and crystallographic data in CIF or other electronic format see DOI: 10.1039/c1ce05387f



**Scheme 1** Preparation of the Ni<sup>II</sup> complexes.

spectroscopy the raw material  $[\text{NiL}_2]$  shows features of the 1,3-*N,S*-coordinated complex  $[\text{Ni}(\text{L-1,3-N,S})_2]$ .

The IR spectrum of the complex  $[\text{Ni}(\text{L-1,3-N,S})_2]$  contains a band at 616 cm<sup>-1</sup> for the P=S group of the anionic forms L. This band is shifted to low frequencies in the spectrum of the complex  $[\text{Ni}(\text{L-1,5-S,S}')_2] \cdot (\text{CH}_3)_2\text{C}=\text{O}$  and was observed at 594 cm<sup>-1</sup>. In the spectra there is a band at 1515–1562 cm<sup>-1</sup>, corresponding to the conjugated SCN fragment. In addition, there is a broad intense band arising from the POC group at 974–982 cm<sup>-1</sup>. The IR spectra of both isomers contain the characteristic band for the arylNH group at 3218–3323 cm<sup>-1</sup>. Furthermore, the spectrum of the acetone solvate contains an intense band at 1702 cm<sup>-1</sup>, corresponding to the C=O group.

The <sup>31</sup>P{<sup>1</sup>H} NMR spectrum of the raw material in CDCl<sub>3</sub> is rather complicated and contains four signals at 50.7, 53.5, 55.0 and 58.4 ppm. The same was previously observed in the spectra of the complexes  $[\text{Ni}\{\text{RNHC}(\text{S})\text{NP}(\text{S})(\text{O}i\text{Pr})_2\}_2]$  (R = *t*Bu, Ad, Ph, 2-MeC<sub>6</sub>H<sub>4</sub>, 2,6-Me<sub>2</sub>C<sub>6</sub>H<sub>3</sub>, 2,4,6-Me<sub>3</sub>C<sub>6</sub>H<sub>2</sub>) in CD<sub>2</sub>Cl<sub>2</sub> or CDCl<sub>3</sub>.<sup>4d,8,9</sup> The high-field signal corresponds to the *trans*-1,5-*S,S'*-coordination, whereas the second signal is typical for the *trans*-1,3-*N,S*-coordination of the deprotonated ligands.<sup>4d,8,9</sup> In view of the similar intensity and line-width of the two low-field signals, they are diastereotopic and assigned to non-equivalent ligand conformations (boat and chair) of the same *cis*-1,5-*S,S'*-complex isomer.<sup>8</sup> The <sup>31</sup>P{<sup>1</sup>H} NMR spectrum of the raw material in acetone-*d*<sub>6</sub> contains a unique signal at 51.3 ppm, which indicates the exclusive presence of diamagnetic 1,5-*S,S'*-coordinated complex forms.<sup>8</sup>

The <sup>1</sup>H NMR spectrum of the raw material in CDCl<sub>3</sub> contains two main sets of signals, which are obviously due to two dominant types of coordination, whereas there is only one set of signals in the spectrum of the complex in acetone-*d*<sub>6</sub>. The signals of the isopropyl CH<sub>3</sub> protons are observed at 1.14–1.78 ppm, while the aryl CH<sub>3</sub> protons are at 2.90–2.98 ppm. The CHO protons are shown at 4.68–4.98 ppm. The spectrum of the complex in CDCl<sub>3</sub> contains two signals of the NH protons, which are observed at 7.34 and 10.76. The low-field signal is presumably due to the formation of intramolecular hydrogen bonds of the type arylN–H···S=P. The signal for the NH protons in the spectrum of the complex in acetone-*d*<sub>6</sub> is shown at 9.18 ppm, which is also in the low-field region due to the formation of intermolecular hydrogen bonds of arylN–H···O=C(acetone) type. The spectra of the complex in both solvents contain the signals of the benzene rings at 6.52–7.37 ppm.

The complexes  $[\text{Ni}(\text{L-1,3-N,S})_2]$  and  $[\text{Ni}(\text{L-1,5-S,S}')_2] \cdot (\text{CH}_3)_2\text{C}=\text{O}$  crystallize in the triclinic space group  $P\bar{1}$  (see ESI†). The complex  $[\text{Ni}(\text{L-1,3-N,S})_2]$  contains four independent molecules in the unit cell. In the complexes, the metal is found to be in a square planar *trans*-N<sub>2</sub>S<sub>2</sub> ( $[\text{Ni}(\text{L-1,3-N,S})_2]$ ) environment formed by the C=S sulfur atoms and the P–N nitrogen atoms (Fig. 1), or in a square planar *trans*-S<sub>2</sub>S'<sub>2</sub> ( $[\text{Ni}(\text{L-1,5-S,S}')_2] \cdot (\text{CH}_3)_2\text{C}=\text{O}$ ) environment formed by the C=S and P=S sulfur atoms of two deprotonated ligands (Fig. 2). The four-membered Ni–S–C–N metallacycles are planar in  $[\text{Ni}(\text{L-1,3-N,S})_2]$ . The six-membered Ni–S–C–N–P–S metallacycles in the acetone solvate have an asymmetric boat form. The values of the intracyclic S–Ni–N angles in the four-membered rings of  $[\text{Ni}(\text{L-1,3-N,S})_2]$  fall in the range of 74–75°, while the intracyclic S–Ni–S angles in  $[\text{Ni}(\text{L-1,5-S,S}')_2] \cdot (\text{CH}_3)_2\text{C}=\text{O}$  are about 99° (Tables S1 and S2 in the ESI†). Inspection of the C=S and P–N bond lengths of  $[\text{Ni}(\text{L-1,3-N,S})_2]$  indicates, that these bonds are best described as single bonds, whereas the P=S distance indicates the presence of a double bond (Table S1 in the ESI†).<sup>3</sup> The lengthening of the C=S and shortening of the C–N bonds are observed upon the  $[\text{Ni}(\text{L-1,5-S,S}')_2] \cdot (\text{CH}_3)_2\text{C}=\text{O}$  complex formation compared to the NTT ligands.<sup>3</sup> The same change, but to a lesser degree, has been observed for the P–N and P=S bonds. The arylNH protons in  $[\text{Ni}(\text{L-1,3-N,S})_2]$  are involved in intramolecular hydrogen bonds of the N–H···S=P type (Table S3 in ESI†). Due to their formation, a flat *syn,syn*-conformation of the N–C–N–P–S unit is favored. The arylNH protons in  $[\text{Ni}(\text{L-1,5-S,S}')_2] \cdot (\text{CH}_3)_2\text{C}=\text{O}$  are also involved in hydrogen bonds (Table S3 in ESI†). The intermolecular hydrogen bonds of the N–H···O=C type are formed between the hydrogen atom of the NH group and the oxygen atom of the acetone molecule, which is trapped during the crystallization. Due to these intermolecular hydrogen bonds the NH hydrogen atom is blocked and, hence, is not suitable for the formation of the intramolecular H-bonding of the N–H···S=P type, permitting the realization of the 1,3-*N,S*-coordination mode of the ligand towards Ni<sup>II</sup>.

Dissolving the raw material in CH<sub>2</sub>Cl<sub>2</sub> and acetone leads to violet and greenish–blue solutions, respectively. The UV-Vis absorption spectra in both solvents contain two bands in the UV region, one lying invariantly at 237–248 nm, the other around 315 nm. However, the latter band in the acetone solution shows a considerably low intensity compared to that in the dichloromethane solution. Absorption bands for the free and protonated ligand RC(S)NHP(X) (O*i*Pr)<sub>2</sub> (X = O, S) are rather high in energy ( $\lambda_{\text{max}}^{\text{abs}} < 250$  nm), while

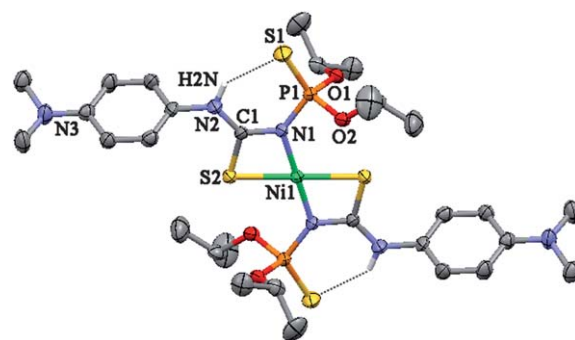


**Fig. 1** Thermal ellipsoid (50%) plot of one of the independent molecules of  $[\text{Ni}(\text{L-1,3-N,S})_2]$ . H-atoms not involved in hydrogen bonding have been omitted for clarity.

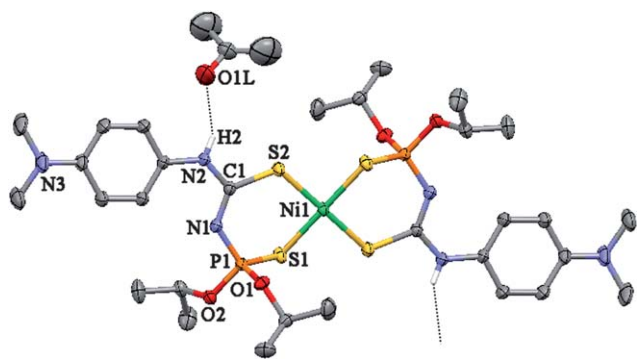


**Fig. 2** Thermal ellipsoid (50%) plot of  $[\text{Ni}(\text{L-1,5-S,S}')_2] \cdot (\text{CH}_3)_2\text{C}=\text{O}$ . H-atoms not involved in hydrogen bonding have been omitted for clarity.

the absorption band of **KL** was observed at 289 nm ( $\epsilon = 184 \text{ M}^{-1} \text{ cm}^{-1}$ ), and have been assigned to intraligand transitions.<sup>8b,10</sup> Thus, the UV absorptions of the nickel complexes can be assigned to corresponding intraligand transitions ( $\pi-\pi^*$  or  $n-\pi^*$  type). The different behaviour of the complexes might be explained by the presence of a mixture of 1,3-*N,S*- and 1,5-*S,S'* isomers in the reaction product in  $\text{CH}_2\text{Cl}_2$  (as evidenced from NMR measurements) while for the complex in acetone exclusively the 1,5-*S,S'* isomer was present. In the visible region essentially two absorption bands were observed, one ranging from 512 to 542, and another being rather invariant at about 650 nm (see ESI†). Due to the rather low intensities ( $172\text{--}201 \text{ M}^{-1} \text{ cm}^{-1}$ ) of the two long-wavelength bands, they are assigned to ligand field (d-d) transitions. For a square planar  $3d^8$  system three bands [ $^1\text{A}_{1g} \rightarrow ^1\text{B}_{1g}$  ( $d_{x^2-y^2} \rightarrow d_{xy}$ ),  $^1\text{A}_{1g} \rightarrow ^1\text{B}_{3g}$  ( $d_{xz} \rightarrow d_{xy}$ ), and  $^1\text{A}_{1g} \rightarrow ^1\text{B}_{1g}$  ( $d_{z^2} \rightarrow d_{xy}$ ), assuming the orbital ordering:  $d_{xy} > d_{x^2-y^2} > d_{yz} > d_{xz} > d_{z^2}$ ] are expected.<sup>3a,6b,9a,11</sup> However comparison with spectra of related complexes suggest that the third band is hidden under the tail of the intense intraligand bands. The assumption that the complex is exclusively 1,5-*S,S'* configured in acetone, while the dichloromethane solution contains both 1,3-*N,S* as well as 1,5-*S,S'* isomers is strongly supported by the absorption spectra of the recently reported derivatives  $[\text{Ni}\{\text{RC}(\text{S})\text{NHP}(\text{X})(\text{O}(\text{Pr})_2)_2\}]$  ( $\text{X} = \text{S}, \text{R} = \text{H}_2\text{N}, \text{MeNH}, t\text{BuNH}, \text{PhNH}, \text{Me}_2\text{N}, 2\text{-MeC}_6\text{H}_4\text{NH}, 2,6\text{-Me}_2\text{C}_6\text{H}_3\text{NH}, 2,4,6\text{-Me}_3\text{C}_6\text{H}_2\text{NH}, 2\text{-Py}(6\text{-Me})\text{NH}; \text{X} = \text{O}, \text{R} = \text{PhNH}$ ).<sup>4a,6,7,8b,9</sup>

The electrochemistry of the raw material was measured using cyclic voltammetry (Table 1). The voltammogram of the complex in  $\text{CH}_2\text{Cl}_2$  differs from that in acetone. This is obviously due to the presence of a mixture of 1,3-*N,S* and 1,5-*S,S'* isomers in  $\text{CH}_2\text{Cl}_2$ , while the exclusively 1,5-*S,S'* isomer is observed in acetone (see NMR data). A reversible first one-electron reduction at about  $-1.50 \text{ V}$  is

**Table 1** Selected electrochemical data for the nickel complex in  $\text{CH}_2\text{Cl}_2$  (upper line) and acetone (bottom line)<sup>a</sup>

$E_{\text{pa}}$ (Ox 3)	$E_{\text{pa}}$ (Ox 2)	$E_{\text{pa}}$ (Ox 1)	$E_{\text{pa}}$ (Red 1)	$E_{\text{pc}}$ (Red 1)	$E_{1/2}$ (Red 1)
—	1.17	0.73	-1.39	-1.51	-1.45
0.71	0.37	-0.04	-1.34	-1.46	-1.40

<sup>a</sup> From cyclic voltammetry in 0.1 M  $n\text{Bu}_4\text{NPF}_6/\text{solvent}$  solutions at  $100 \text{ mV s}^{-1}$  scan rate. Potentials in V vs.  $\text{Fc}/\text{Fc}^+$ . Half-wave potentials  $E_{1/2}$  for reversible processes, peak potential differences  $\Delta E_{\text{pp}} = E_{\text{pa}} - E_{\text{pc}}$  in mV in parentheses (the value for ferrocene was 68 mV), cathodic peak potentials  $E_{\text{pc}}$  and anodic peak potentials  $E_{\text{pa}}$ .

followed by a number of further irreversible reduction steps. This first reduction wave is caused by a ligand-centred reduction.<sup>8b</sup> On the oxidative side of the cyclic voltammogram of the complex in  $\text{CH}_2\text{Cl}_2$  the first wave occurs at  $+0.73 \text{ V}$  (Ox 1) followed by a second at  $+1.17 \text{ V}$  (Ox 2). Measurements of the complex in acetone reveal oxidation processes having very similar potential at  $+0.71 \text{ V}$  (Ox 3). At  $+0.37 \text{ V}$  (Ox 2) there is seemingly an additional oxidation wave. The oxidation is attributed also to a ligand-centred process since the observed vast difference in oxidation potentials for the assumed isomers is too large to be attributed to a nickel-centred oxidation  $\text{Ni}^{\text{II}}/\text{Ni}^{\text{III}}$ . The assumption of a ligand-based oxidation is also in line with the absorption spectroscopy which gave no evidence for a metal-to-ligand or ligand-to-metal charge transfer. Instead, rather low-energy intraligand transitions were observed alongside with low-lying d-d transitions. These observations appeared to be in line with the theoretical TD-DFT study which will be presented hereafter.

In order to study the relative energy of the possible isomers  $[\text{Ni}(\text{L-1,3-*N,S*})_2]$ ,  $[\text{Ni}(\text{L-1,5-*S,S'*})_2]$  and  $[\text{Ni}(\text{L-1,5-*S,S'*})_2] \cdot (\text{CH}_3)_2\text{C}=\text{O}$ , DFT/LanL2DZ calculations were performed at the B3LYP level, as implemented in the Gaussian 09 package.<sup>12</sup> We found true minima on the potential energy surface (PES) for the complexes  $[\text{Ni}(\text{L-1,3-*N,S*})_2]$  and  $[\text{Ni}(\text{L-1,5-*S,S'*})_2]$  exhibiting the following conformations: (i) *trans*-1,3-*N,S* ( $\Delta E = 0.0 \text{ kcal mol}^{-1}$ ), (ii) *cis*-1,3-*N,S* ( $\Delta E = 12.8 \text{ kcal mol}^{-1}$ ), (iii) *trans*-1,5-*S,S'* ( $\Delta E = 17.3 \text{ kcal mol}^{-1}$ ) and (iv) *cis*-1,5-*S,S'* ( $\Delta E = 21.9 \text{ kcal mol}^{-1}$ ) (Fig. S1 in the ESI†). The coordination in a *trans*-1,3-*N,S*-fashion appeared to be more preferred over the *trans*-1,5-*S,S'* conformation when no hydrogen bonding with the acetone molecule is involved in the latter case. The 1,5-*S,S'* isomer must obviously contain an extra stabilization originating from the acetone molecule attached to the hydrogen atom of the NH group (Fig. 2). We have found that the formation of one hydrogen bonding,  $(\text{CH}_3)_2\text{C}=\text{O} \cdots \text{H-N}$ , adds an extra stabilization in the 1,5-*S,S'* system of  $9.2 \text{ kcal mol}^{-1}$ , as compared to the isolated  $[\text{Ni}(\text{L-1,5-*S,S'*})_2]$  complex (Fig. S1 in ESI†). Keeping in mind that two such interactions can be present, it provides a total stabilization of  $18.4 \text{ kcal mol}^{-1}$ . Accordingly, it makes the 1,5-*S,S'* isomer more stable (by  $1.1 \text{ kcal mol}^{-1}$ ) as compared to the *trans*-1,3-*N,S* system (Fig. S1 in ESI†), which can explain why the 1,5-*S,S'* isomer was predominantly observed in acetone.

Finally, we will shed a light on the bonding character between the amine group,  $p\text{-Me}_2\text{NC}_6\text{H}_4\text{NH}$ , and the Ni-containing fragment in the complexes  $[\text{Ni}(\text{L-1,3-*N,S*})_2]$ ,  $[\text{Ni}(\text{L-1,5-*S,S'*})_2]$  and  $[\text{Ni}(\text{L-1,5-*S,S'*})_2] \cdot (\text{CH}_3)_2\text{C}=\text{O}$ . The bonding analysis was performed using the ETS-NOCV scheme<sup>13-15</sup> as implemented in the Amsterdam Density Functional (ADF) package, version 2009.01.<sup>16</sup> The details of the ETS-NOCV scheme are outlined in the ESI†. The fragmentation method used in the bonding analysis is given in Fig. 3 (panel a). It is clear that the amine bonding is the weakest in the case of the  $[\text{Ni}(\text{L-1,5-*S,S'*})_2]$  system ( $\Delta E_{\text{total}} = -86.2 \text{ kcal mol}^{-1}$ ). The main contribution, exhibiting the formation of  $\sigma(\text{HN-C})$  bonding, originates from the charge transfer  $\Delta\rho_1$  (Fig. 3, panel c). It corresponds to  $\Delta E_{\text{orb}}(1) = -390.8 \text{ kcal mol}^{-1}$ . The  $\pi$ -component of the N-C bond,  $\Delta\rho_2$ , is quantitatively far less important,  $\Delta E_{\text{orb}}(1) = -9.3 \text{ kcal mol}^{-1}$ .

As we go from  $[\text{Ni}(\text{L-1,5-*S,S'*})_2]$  to the acetone containing derivative,  $[\text{Ni}(\text{L-1,5-*S,S'*})_2] \cdot (\text{CH}_3)_2\text{C}=\text{O}$ , one might notice the significant strengthening of the amine bonding,  $\Delta E_{\text{total}}$  is lower by  $8.7 \text{ kcal mol}^{-1}$  (Table 2). This is predominantly due to the stronger  $\sigma(\text{HN-C})$  and  $\pi(\text{HN-C})$  components, by  $\Delta E_{\text{orb}}(1) = -34.8 \text{ kcal mol}^{-1}$  and by  $\Delta E_{\text{orb}}(1) = -13.2 \text{ kcal mol}^{-1}$ , respectively (Fig. 3, panel d). Another

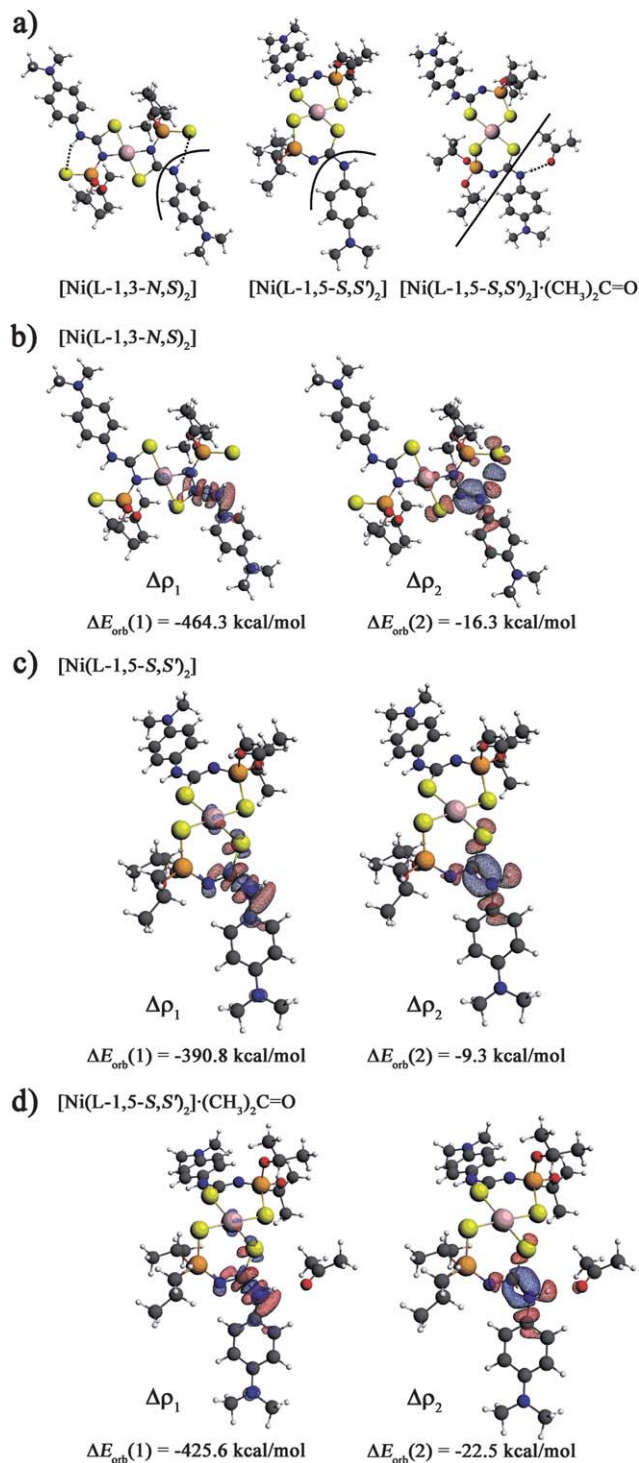


**Fig. 3** Black lines indicate the fragmentation used in the bonding analysis (panel a). In panels b–d the ETS-NOCV based results (deformation densities  $\Delta\rho_i$  and corresponding energies  $\Delta E_{\text{orb}}(i)$ ) are presented for the *trans*-isomers of [Ni(L-1,3-N,S)<sub>2</sub>], [Ni(L-1,5-S,S')<sub>2</sub>] and [Ni(L-1,5-S,S')<sub>2</sub>](CH<sub>3</sub>)<sub>2</sub>C=O, respectively. The red color of the  $\Delta\rho_i$  shows charge depletion, whereas the blue represents charge accumulation upon bond formation. The contour value of 0.005 a.u. was used for  $\Delta\rho_1$ , whereas 0.001 a.u. for  $\Delta\rho_2$ .

**Table 2** ETS-NOCV energy decomposition results (in kcal mol<sup>-1</sup>), describing the interaction between the *p*-Me<sub>2</sub>C<sub>6</sub>H<sub>4</sub>NH group and Ni-based fragments in the *trans*-isomers of [Ni(L-1,3-N,S)<sub>2</sub>] (upper line), [Ni(L-1,5-S,S')<sub>2</sub>] (middle line) and [Ni(L-1,5-S,S')<sub>2</sub>](CH<sub>3</sub>)<sub>2</sub>C=O (bottom line)

$\Delta E_{\text{orb}}$	$\Delta E_{\text{Pauli}}$	$\Delta E_{\text{elstat}}$	$\Delta E_{\text{total}}^a$	$\Delta E_{\text{orb}}(1)$	$\Delta E_{\text{orb}}(2)$
-493.8	693.5	-303.0	-103.3	-464.3	-16.3
-414.3	597.0	-268.9	-86.2	-390.8	-9.3
-474.2	686.6	-307.3	-94.9	-425.6	-22.5

<sup>a</sup>  $\Delta E_{\text{total}} = \Delta E_{\text{orb}} + \Delta E_{\text{Pauli}} + \Delta E_{\text{elstat}}$ .

important factor is the higher stabilization (by 34.8 kcal mol<sup>-1</sup>) originating from the electrostatic term. It should be pointed out that when considering not one, but two acetone molecules, further stabilization of [Ni(L-1,5-S,S')<sub>2</sub>] is expected. Indeed, as it has been already mentioned, an inclusion of two acetone species makes the [Ni(L-1,5-S,S')<sub>2</sub>](CH<sub>3</sub>)<sub>2</sub>C=O<sub>2</sub> system the most stable (Fig. S1 in ESI<sup>†</sup>). Thus, it clearly shows the important role of the solvent (acetone species) environment in controlling the stability of the [Ni(L-1,5-S,S')<sub>2</sub>] complex. In addition, we found that the stabilization originating directly from the formation of hydrogen bonding in [Ni(L-1,5-S,S')<sub>2</sub>](CH<sub>3</sub>)<sub>2</sub>C=O is -5.7 kcal mol<sup>-1</sup> (Fig. S2 in ESI<sup>†</sup>). It is less pronounced than the strengthening of amine bonding caused by the presence of the acetone species (by 8.7 kcal mol<sup>-1</sup>).

In order to gain further insight into the nature of the absorption spectra for the [Ni(L-1,5-S,S')<sub>2</sub>] and [Ni(L-1,3-N,S)<sub>2</sub>] complexes, a time dependent density functional method (TD-DFT) was applied, as implemented in ADF package.<sup>16</sup> The simulated spectrum (at the DFT/B3LYP level of theory) in the gas phase together with the selected molecular orbitals involved in the dominant transitions are presented in Fig. 4 and 5 for [Ni(L-1,5-S,S')<sub>2</sub>] and [Ni(L-1,3-N,S)<sub>2</sub>], respectively.

It can clearly be seen from Fig. 4 (part A) that one dominant band, with the large oscillator strength  $f = 0.7605$  a.u. was obtained at 364 nm in the case of the [Ni(L-1,5-S,S')<sub>2</sub>] isomer. This transition is dominated by a HOMO → LUMO + 1 charge transfer (Fig. 4, part B). It can be noticed qualitatively the charge transfer from the  $\pi$ -type orbital of aryl ring and the lone electron pairs of sulfur (HOMO) and the charge accumulation into the anti-bonding ligand orbitals (both  $\pi^*$  and  $\sigma^*$ ). Minor participation of the metal is noted from the HOMO contour. Another important band, with the oscillator strength  $f = 0.3014$  a.u., is observed at 319 nm (Fig. 4, part A). It involves both the HOMO - 1 → LUMO + 2 (63.5%) and HOMO → LUMO + 3 (30.6%) transitions. Again, they represent primarily the intra-ligand charge transfers with the minor participation of the metal. Among less important transitions in the lower frequency region one can see the two peaks, at 419 nm ( $f = 0.021$  a.u.) and at 500 nm ( $f = 0.038$  a.u.). They originate from HOMO - 5 → LUMO and HOMO → LUMO charge transfers, respectively. In both cases one can conclude from the shape of molecular orbitals (Fig. 4, part B) that these transfers can be attributed to intra-ligand and the metal d-d transitions.

Concerning the spectrum of the [Ni(L-1,3-N,S)<sub>2</sub>] isomer one might notice from Fig. 5 (part A) that the dominant band, with  $f = 0.7484$  a.u., is observed at 337 nm. This transition is constituted, similarly to the [Ni(L-1,5-S,S')<sub>2</sub>] isomer, from the HOMO →

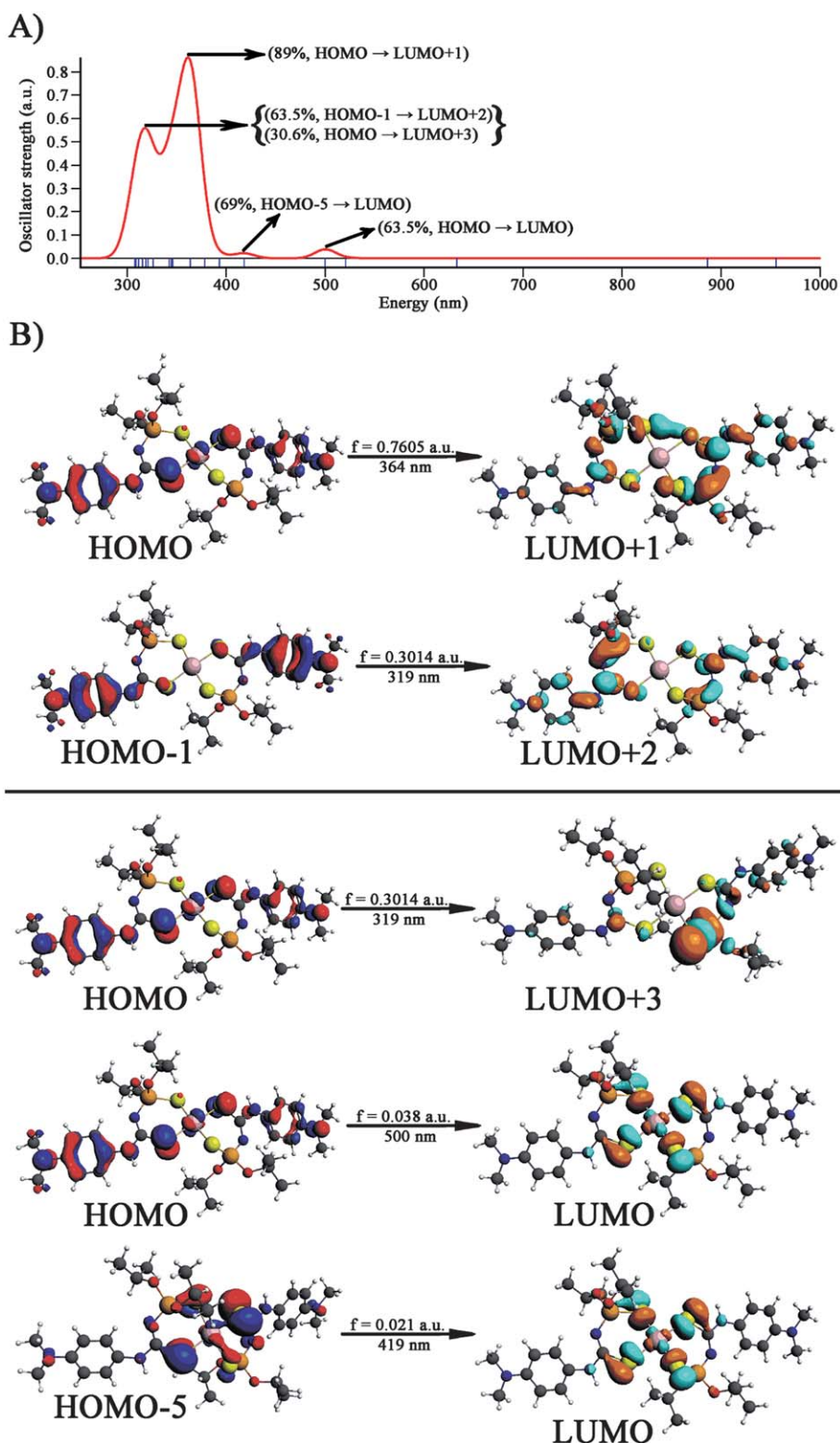


**Fig. 4** Simulated TD-DFT/B3LYP spectrum of the  $[\text{Ni}(\text{L-1,5-S,S}')_2]$  complex in the gas phase (part A) together with the contours of molecular orbitals (0.03 a.u.) involved in the dominant transitions (part B).

LUMO + 1 intra-ligand charge transfer (Fig. 5, part B). Another, far less intense band ( $f = 0.029$  a.u.) at 448 nm involves HOMO - 1 → LUMO charge transfer—it exhibits both the intra-ligand transition (LLCT) with some participation of the metal (LMCT). From

the shape of the LUMO contour, it can be noticed that participation of the metal (thus LMCT) seems to be of less importance as compared to the intra-ligand oxidation (LLCT). Finally, it should be emphasized that evident domination of the intra-ligand oxidation

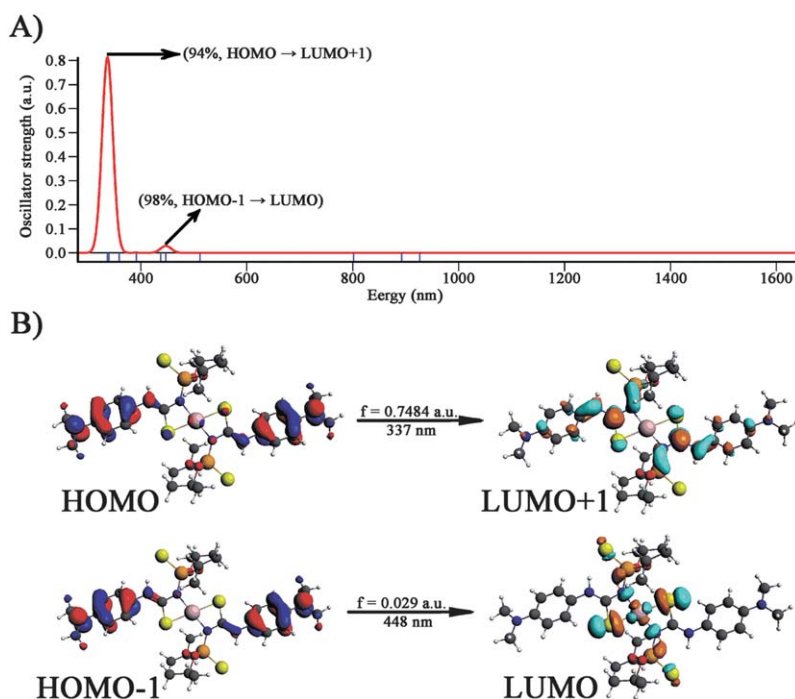


**Fig. 5** Simulated TD-DFT spectrum of  $[\text{Ni}(\text{L-1,3-}N,S)_2]$  system (part A) together with the contours of molecular orbitals (0.03 a.u.) involved in the dominant transitions (part B).

in the case of both isomers is fully in line with the experimental findings based on CV-experiments.

We have synthesized the  $\text{Ni}^{\text{II}}$  complexes  $[\text{Ni}\{p\text{-Me}_2\text{NC}_6\text{H}_4\text{HNC}(\text{S})\text{NP}(\text{S})(\text{O}i\text{Pr})_2\text{-1,3-}N,S\}_2]$ ,  $[\text{Ni}(\text{L-1,3-}N,S)_2]$ , and  $[\text{Ni}\{p\text{-Me}_2\text{NC}_6\text{H}_4\text{HNC}(\text{S})\text{NP}(\text{S})(\text{O}i\text{Pr})_2\text{-1,5-}S,S'\}_2] \cdot (\text{CH}_3)_2\text{C}=\text{O}$ ,  $[\text{Ni}(\text{L-1,5-}S,S')_2] \cdot (\text{CH}_3)_2\text{C}=\text{O}$ . These compounds are the first examples of  $\text{Ni}^{\text{II}}$  complexes containing the same asymmetric **NTT** ligand featuring an aryl-NH substituent at the thiocarbonyl group and coordinating to the metal both in the 1,3- $N,S$ - and 1,5- $S,S'$ -fashion in the solid state depending on the crystallization conditions. Finally, comparing the  $[\text{Ni}(\text{L-1,3-}N,S)_2]$  conformation with the  $[\text{Ni}(\text{L-1,5-}S,S')_2]$  and  $[\text{Ni}(\text{L-1,5-}S,S')_2] \cdot (\text{CH}_3)_2\text{C}=\text{O}$  systems, it should be added that the highest stabilization of the former conformation,  $\Delta E_{\text{total}} = -103.3$  kcal  $\text{mol}^{-1}$ , is predominantly related to the strongest  $\sigma(\text{HN-C})$  bonding ( $\Delta E_{\text{orb}}(1) = -464.3$  kcal  $\text{mol}^{-1}$ ) as well as of the intramolecular  $\text{HN} \cdots \text{S}$  interaction ( $\Delta E_{\text{orb}}(2) = -16.3$  kcal  $\text{mol}^{-1}$ ) (Fig. 3, panel a). Another important factor is the large electrostatic stabilization (Table 2).

## Acknowledgements

M. P. Mitoraj greatly acknowledges the financial support from the Foundation for Polish Science ("START" scholarship) as well as from Polish Ministry of Science and Higher Education ("Outstanding Young Researchers" scholarship). M. Srebro also acknowledges the financial support from the Foundation for Polish Science ("START" scholarship). We are also grateful to ACK CYFRONET - Krakow, to the Laboratory of Parallel Computing of the Institute of Computer Science AGH for the computer time and to the F.R.S.-FNRS (Belgium) for financial support (FRFC 2.4.508.08.F) as well as a post-doctoral position to D. A. Safin.

## Notes and references

- For examples: (a) R. Rösler, C. Silvestru, G. Espinosa-Perez, I. Haiduc and R. Cea-Olivares, *Inorg. Chim. Acta*, 1996, **241**, 47; (b) A. Silvestru, D. Bilc, R. Rosler, J. E. Drake and I. Haiduc, *Inorg. Chim. Acta*, 2000, **305**, 106; (c) E. V. Garcia-Baez, M. J. Rozales-Hoz, H. Nöth, I. Haiduc and C. Silvestru, *Inorg. Chem. Commun.*, 2000, **3**, 173; (d) S. D. Robertson, T. Chivers, J. Akhtar, M. Afzaal and P. O'Brien, *Dalton Trans.*, 2008, 7004; (e) I. Haiduc, *J. Organomet. Chem.*, 2001, **623**, 29; (f) A. Panneerselvam, M. A. Malik, M. Afzaal, P. O'Brien and M. Helliwell, *J. Am. Chem. Soc.*, 2008, **130**, 2420; (g) N. Levesanos, S. D. Robertson, D. Maganas, C. P. Raptopoulou, A. Terzis, P. Kyritsis and T. Chivers, *Inorg. Chem.*, 2008, **47**, 2949; (h) D. Maganas, A. Grigoropoulos, S. S. Staniland, S. D. Chatziefthimiou, A. Harrison, N. Robertson, P. Kyritsis and F. Neese, *Inorg. Chem.*, 2010, **49**, 5079; (i) E. Ferentinos, D. Maganas, C. P. Raptopoulou, A. Terzis, V. Psycharis, N. Robertson and P. Kyritsis, *Dalton Trans.*, 2011, **40**, 169.
- For examples: (a) K. R. Koch, O. Hallale, S. A. Bourne, J. Miller and J. Bacsá, *J. Mol. Struct.*, 2001, **561**, 185; (b) S. A. Bourne, O. Hallale and K. R. Koch, *Cryst. Growth Des.*, 2005, **5**, 307; (c) O. Hallale, S. A. Bourne and K. R. Koch, *New J. Chem.*, 2005, **29**, 1416; (d) O. Hallale, S. A. Bourne and K. R. Koch, *CrystEngComm*, 2005, **7**, 161.
- For examples: (a) F. D. Sokolov, V. V. Brusko, N. G. Zabiroy and R. A. Cherkasov, *Curr. Org. Chem.*, 2006, **10**, 27; (b) F. D. Sokolov, V. V. Brusko, D. A. Safin, R. A. Cherkasov and N. G. Zabiroy, Coordination Diversity of *N*-Phosphorylated Amides and Ureas Towards VIII B Group Cations, in *Transition Metal Chemistry: New Research*, ed. B. Varga and L. Kis, 2008, Nova Science Publishers Inc., Hauppauge NY, USA, p. 101 and references therein.
- (a) F. D. Sokolov, N. G. Zabiroy, L. N. Yamalievá, V. G. Shtyrlin, R. R. Garipov, V. V. Brusko, A. Yu. Verat, S. V. Baranov, P. Mlynarz, T. Glowiak and H. Kozłowski, *Inorg. Chim. Acta*, 2006, **359**, 2087; (b) F. D. Sokolov, S. V. Baranov, D. A. Safin, F. E. Hahn, M. Kubiak, T. Pape, M. G. Babashkina, N. G. Zabiroy, J. Galezowska, H. Kozłowski and R. A. Cherkasov, *New J. Chem.*, 2007, **31**, 1661; (c) F. D. Sokolov, S. V. Baranov, N. G. Zabiroy, D. B. Krivolapov, I. A. Litvinov, B. I. Khairutdinov and

- R. A. Cherkasov, *Mendeleev Commun.*, 2007, **17**, 222; (d) D. A. Safin, F. D. Sokolov, M. G. ŁSzyrwiłBabashkina, T. R. Gimadiev, F. E. Hahn, H. Kozłowski, D. B. Krivolapov and I. A. Litvinov, *Polyhedron*, 2008, **27**, 2271; (e) D. A. Safin, M. G. Babashkina, A. Klein, F. D. Sokolov, S. V. Baranov, T. Pape, F. E. Hahn and D. B. Krivolapov, *New J. Chem.*, 2009, **33**, 2443.
- 5 (a) D. A. Safin, F. D. Sokolov, S. V. Baranov, Ł. Szyrwił, M. G. Babashkina, E. R. Shakirova, F. E. Hahn and H. Kozłowski, *Z. Anorg. Allg. Chem.*, 2008, **634**, 835; (b) A. Yu. Verat, V. G. Shtyrln, B. I. Khairutdinov, F. D. Sokolov, L. N. Yamaliev, D. B. Krivolapov, N. G. Zabirow, I. A. Litvinov and V. V. Klochkov, *Mendeleev Commun.*, 2008, **18**, 150.
- 6 (a) D. A. Safin, M. Bolte, M. G. Babashkina and H. Kozłowski, *Polyhedron*, 2010, **29**, 488; (b) D. A. Safin, M. G. Babashkina, M. Bolte and A. Klein, *Inorg. Chim. Acta*, 2011, **365**, 32.
- 7 M. G. Babashkina, D. A. Safin, M. Bolte and A. Klein, *Polyhedron*, 2010, **29**, 1515.
- 8 (a) M. G. Babashkina, D. A. Safin, M. Bolte and A. Klein, *Inorg. Chem. Commun.*, 2009, **12**, 678; (b) M. G. Babashkina, D. A. Safin, M. Bolte, M. Srebro, M. Mitoraj, A. Uthe, A. Klein and M. Köckerling, *Dalton Trans.*, 2011, **40**, 3142.
- 9 (a) V. V. Brusko, A. I. Rakhmatullin, V. G. Shtyrln, D. B. Krivolapov, I. A. Litvinov and N. G. Zabirow, *Polyhedron*, 2006, **25**, 1433; (b) D. A. Safin, F. D. Sokolov, T. R. Gimadiev, V. V. Brusko, M. G. Babashkina, D. R. Chubukaeva, D. B. Krivolapov and I. A. Litvinov, *Z. Anorg. Allg. Chem.*, 2008, **634**, 967.
- 10 (a) D. A. Safin, F. D. Sokolov, H. Nöth, M. G. Babashkina, T. R. Gimadiev, J. Galezowska and H. Kozłowski, *Polyhedron*, 2008, **27**, 2022; (b) D. A. Safin, A. Klein, M. G. Babashkina, H. Nöth, D. B. Krivolapov, I. A. Litvinov and H. Kozłowski, *Polyhedron*, 2009, **28**, 1504; (c) D. A. Safin, M. G. Babashkina, M. Bolte, T. Pape, F. E. Hahn, M. L. Verizhnikov, A. R. Bashirov and A. Klein, *Dalton Trans.*, 2010, **39**, 11577.
- 11 (a) R. H. Dingle, *Inorg. Chem.*, 1971, **10**, 1141; (b) V. V. Brusko, A. I. Rakhmatullin, V. G. Shtyrln and N. G. Zabirow, *Russ. J. Gen. Chem.*, 2000, **70**, 1521.
- 12 M. J. Frisch, G. W. Trucks, H. B. Schlegel, G. E. Scuseria, M. A. Robb, J. R. Cheeseman, G. Scalmani, V. Barone, B. Mennucci, G. A. Petersson, H. Nakatsuji, M. Caricato, X. Li, H. P. Hratchian, A. F. Izmaylov, J. Bloino, G. Zheng, J. L. Sonnenberg, M. Hada, M. Ehara, K. Toyota, R. Fukuda, J. Hasegawa, M. Ishida, T. Nakajima, Y. Honda, O. Kitao, H. Nakai, T. Vreven, J. A. Montgomery Jr., J. E. Peralta, F. Ogliaro, M. Bearpark, J. J. Heyd, E. Brothers, K. N. Kudin, V. N. Staroverov, R. Kobayashi, J. Normand, K. Raghavachari, A. Rendell, J. C. Burant, S. S. Iyengar, J. Tomasi, M. Cossi, N. Rega, J. M. Millam, M. Klene, J. E. Knox, J. B. Cross, V. Bakken, C. Adamo, J. Jaramillo, R. Gomperts, R. E. Stratmann, O. Yazyev, A. J. Austin, R. Cammi, C. Pomelli, J. W. Ochterski, R. L. Martin, K. Morokuma, V. G. Zakrzewski, G. A. Voth, P. Salvador, J. J. Dannenberg, S. Dapprich, A. D. Daniels, Ö. Farkas, J. B. Foresman, J. V. Ortiz, J. Ciosłowski and D. J. Fox, *Gaussian 09*, Gaussian Inc., Wallingford CT, 2009.
- 13 M. Mitoraj and A. Michalak, *J. Mol. Model.*, 2007, **13**, 347.
- 14 M. Mitoraj, A. Michalak and T. Ziegler, *J. Chem. Theory Comput.*, 2009, **5**, 962.
- 15 M. Mitoraj and A. Michalak, *Inorg. Chem.*, 2011, **50**, 2168.
- 16 (a) G. te Velde, F. M. Bickelhaupt, E. J. Baerends, C. Fonseca Guerra, S. J. A. van Gisbergen, J. G. Snijders and T. Ziegler, *J. Comput. Chem.*, 2001, **22**, 931; (b) ADF2009.01: E. J. Baerends, J. Autschbach, D. Bashford, A. Bérces, F. M. Bickelhaupt, C. Bo, P. M. Boerrigter, L. Cavallo, D. P. Chong, L. Deng, R. M. Dickson, D. E. Ellis, M. van Faassen, L. Fan, T. H. Fischer, C. Fonseca Guerra, A. Ghysels, A. Giammona, S. J. A. van Gisbergen, A. W. Götz, J. A. Groeneveld, O. V. Gritsenko, M. Grüning, F. E. Harris, P. van den Hoek, C. R. Jacob, H. Jacobsen, L. Jensen, G. van Kessel, F. Kootstra, M. V. Krykunov, E. van Lenthe, D. A. McCormack, A. Michalak, M. Mitoraj, J. Neugebauer, V. P. Nicu, L. Noodleman, V. P. Osinga, S. Patchkovskii, P. H. T. Philipsen, D. Post, C. C. Pye, W. Ravenek, J. I. Rodríguez, P. Ros, P. R. T. Schipper, G. Schreckenbach, M. Seth, J. G. Snijders, M. Solà, M. Swart, D. Swerhone, G. te Velde, P. Vernooijs, L. Versluis, L. Visscher, O. Visser, F. Wang, T. A. Wesolowski, E. M. van Wezenbeek, G. Wiesenekker, S. K. Wolff, T. K. Woo, A. L. Yakovlev and T. Ziegler, Theoretical Chemistry, Vrije Universiteit, Amsterdam.